Geomagnetic Storm Simulation With a Coupled Magnetosphere–Ionosphere–Thermosphere Model

Joachim Raeder

Institute of Geophysics and Planetary Physics, University of California, Los Angeles, California

Yongli Wang

Department of Earth and Space Sciences, University of California, Los Angeles, California

Timothy J. Fuller-Rowell

NOAA Space Environment Center, Boulder, Colorado
CIRES, University of Colorado

Abstract.
We present the first global, self-consistent, fully electrically coupled magnetosphere–ionosphere–thermosphere model, based on the UCLA magnetosphere–ionosphere model and the NOAA Coupled Thermosphere Ionosphere Model (CTIM). Initial results from this coupled model for the January 10, 1997 geomagnetic storm event are encouraging. In particular, the model produces a much more realistic electrodynamic and ionospheric response as compared with the previous magnetosphere model that relied on parameterizations for the ionospheric conductance. This is attributed to the much more realistic conductance calculations provided by CTIM. Like in previous studies with the magnetosphere model, the cross-polar-cap potential is too high. Examining the cause will require further investigation.

1. INTRODUCTION

Contemporary terrestrial weather forecasts rely on a combination of dense observation networks and sophisticated numerical models which project the current weather conditions into the future. Similarly, space weather forecasting will require large scale numerical models of Earth's space environment as a key operational element, along with sufficient timely observations to provide model input and to initialize model fields. Besides their utility for space weather forecasting, such models are also essential tools to understand the environment and the plasma physical processes in it, because *in situ* measurements are often too sparse to enable a unique interpretation of the data, and because the complexity of the space environment limits our theoretical understanding. By comparing predictions with data, large scale models also serve to test our knowledge about the prevailing processes, i.e., successful model predictions suggest that the assumptions underlying the model are correct, whereas model failures point to deficiencies of our understanding. Models have also become an increasingly important tools to analyze and interpret experimental data, by putting *in situ* measurements from a single (or at most a few) spacecraft into perspective and thus extending the "view" of the observations. Thus, progress is often made by combining data analysis with global modeling, since both are essentially complementary. In the foreseeable future tens to hundreds of spacecraft might provide data, in which case models will play a crucial role in assimilating these measurements in order to provide global synoptic maps of Earth's space environment.

No global comprehensive model of Earth's space environment exists today. However, regional models have been developed that treat limited regions or processes. For example, global MHD models cover the outer magnetosphere [*Lyon et al.*, 1998; *Ogino*, 1986; *Winglee and Menietti*, 1998; *Gombosi et al.*, 1998; *Tanaka*, 1995; *Janhunen et al.*, 1995; *Raeder*, 1999], but omit the particle drift physics of the inner magnetosphere within a few R_E from Earth as well as the plasma and neutral constituents of the ionosphere–thermosphere system. Some of these models [*Lyon et al.*,

1998; *Tanaka*, 1995; *Janhunen et al.*, 1995; *Raeder*, 1999] include an ionosphere submodel that solves a potential equation to close the field aligned currents originating in the magnetosphere. The ionospheric conductance in these submodels is either taken to be constant or derived by using empirical models for EUV ionization and parameterizations for electron precipitation in the auroral zone [e.g. *Slinker et al.*, 1998; *Raeder*, 1999]. However, such submodels do not fully represent the ionosphere–thermosphere system, but approximate only one aspect of it, namely the closure of field aligned currents, and rely on a number of approximations and parameterizations.

On the other hand, fully dynamical models of the ionosphere–thermosphere system exist, for example the Thermosphere Ionosphere Mesosphere Electrodynamics General Circulation Model (TIME-GCM) [*Roble and Ridley*, 1994] or the NOAA Coupled Thermosphere Ionosphere Model (CTIM) [*Fuller-Rowell et al.*, 1996]. These models depend on magnetospheric input, for example the electric field and particle precipitation. For the lack of direct observations of these quantities with sufficient resolution, they are usually taken from empirical (climatological) models, parameterizations, or data-assimilative models, for example AMIE [*Richmond and Kamide*, 1988].

Clearly, comprehensive models of Earth's space environment require the coupling of magnetosphere models with ionosphere–thermosphere models because these types of models are complementary. The global magnetosphere models lack the physical first-principle calculations at the ionospheric end which can be provided by an ionosphere–thermosphere (IT) model; vice versa, IT models require input that magnetosphere models can provide, and at the same time provide input to magnetosphere models.

In this paper we present the first attempt of producing such a coupled model consisting of the UCLA global magnetosphere model with the NOAA CTIM model. In the following sections we briefly describe the two models, discuss the coupling issues, and present some initial results from the coupled model.

2. THE UCLA GLOBAL MAGNETOSPHERE MODEL

The UCLA global magnetosphere model solves the MHD equations in a large volume surrounding Earth such that the entire interaction region between the solar wind and the magnetosphere is included. Specifically, the simulation domain comprises the bow shock, magnetopause, and the magnetotail up to several hundred R_E from Earth. Thus the model input is given by the solar wind plasma and IMF (Interplanetary Magnetic Field), which for most studies (and space weather applications) is taken from measurements of a solar wind monitor such as WIND or ACE. This model has been developed and continually improved over the many years and now goes well beyond a "three-dimensional global MHD simulation model". Besides numerically solving the MHD equations with high spatial resolution, the model also includes ionospheric processes and their electrodynamic coupling with the magnetosphere. The coupling between the magnetosphere and the ionosphere is an essential part of the model because the ionosphere controls to a large part magnetospheric convection, by providing the resistive closure of the field aligned currents that are generated from the interaction of the solar wind with the magnetosphere [*Raeder et al.*, 1998]. Processes that occur in the near-Earth region on polar cap and auroral field lines and that are inherently kinetic have been parameterized in the model using empirical relationships [*Raeder et al.*, 2001]. These processes include the field aligned potential drops that are associated with upward field aligned currents and related electron precipitation, and the diffuse electron precipitation that is caused by pitch angle scattering of plasma sheet electrons [*Lyons et al.*, 1979; *Weimer et al.*, 1987; *Kennel and Petschek*, 1966]. In previous simulations the electron precipitation parameters were used to determine the ionospheric Pedersen and Hall conductances using the empirical *Robinson et al.* [1987] formulae, while the new model uses CTIM conductances (see below). The model uses the conductances and the field aligned currents to solve the ionospheric potential equation. The embedded ionosphere model yields many ionospheric quantities that are observable from the ground and low Earth orbiting satellites. The primary quantities are the field aligned currents, the Hall and Pedersen conductance, and the electric potential. From these, other related quantities are derived, such as the total and equivalent ionospheric current, dissipation rates, and ground magnetic perturbations. In particular, the ground magnetic perturbation can be computed at any point of the auroral zone and the polar cap, as well as related geomagnetic indices like the AE, AU, and AL indices. The availability of the synthetic magnetograms and indices allows for direct comparisons with ground data [*Raeder et al.*, 2001] and are of great significance for space weather.

The numerical grid is rectangular and nonuniform with the highest spatial resolution (about 0.3 R_E) near Earth and in the tail plasma sheet. It extends about 20 R_E in the sunward direction, 300 R_E in the tailward direction and ± 40 R_E in the Y and Z directions. The gas-dynamic part of the MHD equations is spatially differenced by using a technique in which fourth-order fluxes are hybridized with first-order (Rusanov) fluxes [*Harten and Zwas*, 1972; *Hirsch*, 1990]. The magnetic induction equation is treated some-

what differently [*Evans and Hawley*, 1988] in order to conserve $\nabla \cdot \mathbf{B} = 0$ exactly. The time stepping scheme for all variables consists of a low-order predictor with a time-centered corrector, which is accurate to the second order in time. Thus, the numerical scheme is flux-limited, i.e., it produces diffusion only to the extent needed at shocks and discontinuities. In regions where all variables vary smoothly, the gas dynamic variables are computed with fourth-order accuracy, and the magnetic field with second-order accuracy. The outer boundary conditions are fixed at the given solar wind values on the upstream side. At the other boundaries we apply open, i.e., zero normal derivative, boundary conditions. For optimal performance the code is parallelized for state-of-the-art massively parallel computers (IBM-SP2, SGI-O2000, Beowulf Clusters) using domain decomposition [*Fox et al.*, 1988] and MPI message passing. Real time operation with a grid of about 10^6 cells takes about 40 processors of either of these computers. A more detailed description of the model can be found in [*Raeder*, 1999; *Raeder et al.*, 2001].

3. THE NOAA COUPLED IONOSPHERE THERMOSPHERE MODEL

CTIM is a global multi-fluid model of the thermosphere–ionosphere system with a long heritage [see *Fuller-Rowell et al.*, 1996, and references therein]. CTIM solves both neutral and ion fluid equations self-consistently from 80 to 500 km for the neutral atmosphere and from 80 to 10,000 km for the ionosphere on a spherical grid with 2° latitude resolution and 18° longitude resolution. The thermosphere part solves the continuity equation, horizontal momentum equation, energy equation, and composition equations for the major species O, O_2, and N_2 on 15 pressure levels. The ionosphere model part solves the continuity equations, ion temperature equation, vertical diffusion equations, and horizontal transport for H^+ and O^+, while chemical equilibrium is assumed for N_2^+, O_2^+, NO^+, and N^+. The horizontal ion motion is governed by the magnetospheric electric field. The coupled model includes about 30 different chemical and photo-chemical reactions between the species. Compared to the magnetosphere, the CTIM timescales are relatively long, allowing for numerical timesteps of the order of 1 minute. Consequently, CTIM is computationally very efficient and runs considerably faster than real-time (>10 times) on a single CPU.

CTIM's primary inputs are the solar UV and EUV fluxes (parameterized by the solar 10.7 cm radio flux), the tidal modes (forcing from below), auroral precipitation, and the magnetospheric electric field, each of which is usually taken from parameterized empirical models.

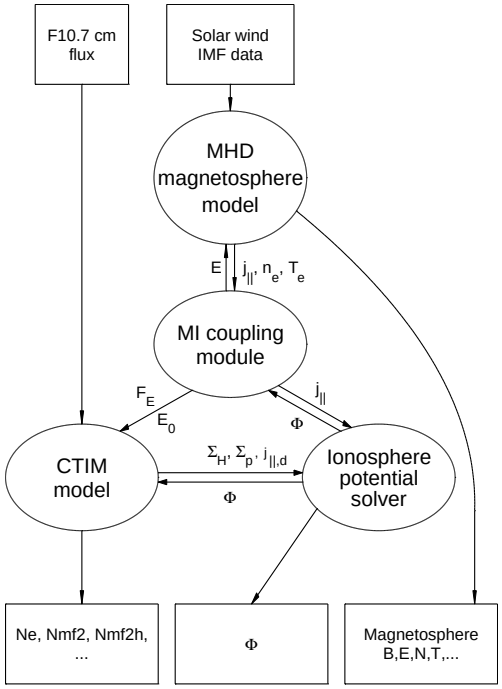

Figure 1. Schematic of the coupled magnetosphere–ionosphere–thermosphere model. The arrows represent the data flow.

CTIM provides several outputs that are of prime importance for space weather, for example global two- and three-dimensional ionosphere and thermosphere state fields, like electron density, neutral density, neutral wind, chemical composition, NmF2, hmF2, and total electron content (TEC). Specifically, the electron parameters are important because they strongly affect HF communication and navigation systems, and the neutral densities are important because they determine the drag on LEO satellites and space debris.

A more thorough description of CTIM, including the detailed equations, reaction rates, and examples can be found in [*Fuller-Rowell et al.*, 1996].

4. COUPLING ISSUES

Figure 1 shows schematically how the magnetosphere model and CTIM are coupled. The “MI coupling module” and the “ionosphere potential solver” are part of the magnetosphere model. Specifically, the MI coupling module maps field aligned currents from the magnetosphere to the ionosphere and computes electron precipitation fluxes (F_E) and

mean energies (E_0). In the opposite direction, it maps the ionospheric electric field to the inner boundary of the magnetosphere model (which is a sphere of about 3-4 R_E radius centered on Earth) where it is used as an MHD boundary condition [*Raeder*, 1999; *Raeder et al.*, 2001]. The potential solver solves the ionosphere potential equation

$$\nabla \cdot \Sigma \cdot \nabla \Phi = -j_{\parallel} \sin I + j_{\parallel,d}$$

on the surface of a sphere with 1.015 R_E radius. Here, Φ is the ionosphere potential, Σ is the conductance tensor, $j_{\parallel}$ is the magnetospheric field aligned current (FAC), $j_{\parallel,d}$ is a parallel current arising from the ionospheric dynamo, and I is the magnetic field inclination in the ionosphere. The ionospheric dynamo current $j_{\parallel,d}$ arises from the ion-neutral drag in the ionosphere, in which the electric field $\mathbf{E}'$ in the reference frame of the neutrals is given by $\mathbf{E}' = \mathbf{E} + \mathbf{U}\times\mathbf{B}$ [*Kelley*, 1989] where $\mathbf{U}$ is the velocity of the neutrals. From $\nabla \cdot \mathbf{J} = 0$ and $\mathbf{J} = \sigma \cdot \mathbf{E}'$ follows by integration over z:

$$j_{\parallel,d} = -\nabla \cdot \int_z \sigma \cdot (\mathbf{U}\times\mathbf{B}) dz$$

where σ is the conductivity tensor and $\mathbf{B}$ is the magnetic field.

In coupling the magnetosphere model with CTIM, the MI coupling module provides the electron precipitation parameters and the magnetospheric electric field. In turn, CTIM provides the ionospheric conductance and $j_{\parallel,d}$ to the potential solver. Thus, as far as the magnetosphere model is concerned, we replace empirical conductance calculations [*Robinson et al.*, 1987] with first-principle calculations and also account for the ionospheric dynamo effect. The latter effect is probably of minor importance in most situations, but may become significant during storm recovery [*Richmond and Roble*, 1987]. With this coupling, CTIM is also driven with more realistic magnetospheric inputs and depends on fewer empirical parameters.

Because the ionosphere–thermosphere time scales are significantly slower than the magnetospheric time scales the computational coupling between the models can be relatively loose. Typical numerical timesteps for the MHD model are about 0.2 to 0.5 seconds, whereas a typical CTIM timestep takes about 60 seconds. Thus CTIM is only invoked every 60 seconds, and for the MHD timesteps between CTIM invocations the parameters Σ and $j_{\parallel,d}$ are held constant in the magnetosphere model. Moreover, CTIM runs on a separate computational node asynchronously from the MHD calculations, i.e., after CTIM receives parameters from the magnetosphere model, it returns immediately Σ and $j_{\parallel,d}$ from its last step. This makes the calculations much more efficient because the magnetosphere model needs not to wait for CTIM to finish. Thus the CTIM calculation lags the magnetosphere calculations by 60 seconds. However, this time is at least partially compensated for by the instantaneous mapping of quantities between the MHD boundary and the ionosphere, which in reality takes a finite amount of time.

5. MODEL COMPARISONS FOR THE JANUARY 10/11, 1997 GEOMAGNETIC STORM

The magnetic storm of January 10/11, 1997 has been discussed in substantial detail in the literature [see for example: *Fox et al.*, 1998; *Goodrich et al.*, 1998; *Spann et al.*, 1998], thus we refer the reader to these papers regarding the specifics of this event. Briefly, a magnetic cloud encountered Earth's magnetosphere at 0441 UT on 1/10/1997, following a storm sudden commencement at 0050 UT on the same day. The IMF B_z associated with the cloud turned initially southward and stayed southward for the next 12 hours. Associated with the southward IMF was strong geomagnetic activity. The Canopus electrojet CL index [*Rostoker et al.*, 1995; *Goodrich et al.*, 1998] reached values of -1800 nT, and the Polar UVI imager recorded strong auroral emissions throughout this period [*Spann et al.*, 1998]. *Lu et al.* [1999] presented a study of this storm in which they used AMIE [*Richmond and Kamide*, 1988] and DMSP data to estimate ionospheric power inputs and the cross polar cap potential. In the following we use results from this study to compare three different simulation runs with data and with each other.

In run 1 we used the simplest ionosphere model possible, namely a flat ionospheric conductance of 5 S. With a flat conductance model we do not expect significant perturbations of the ground magnetic field. As shown by *Fukushima* [1969, 1975, see also *Kamide et al.* 1981] the ground magnetic effects of the field-aligned and the poloidal ionospheric currents cancel. Because there is no toroidal ionospheric current for a flat conductance model, only minor ground perturbations are expected. These arise from the deviations of our model from the idealizations in Fukushima's theorem, namely a radial magnetic field and an infinite ionosphere.

Results from this run are shown in Figure 2. Here, we focus on the first 10 hours of the cloud event during which most of the auroral activity occurred. The figure shows, from top to bottom, the IMF B_z and the solar wind number density measured by Wind for reference (not time shifted), the Canopus CL index, the cross-polar-cap potential in the northern hemisphere, and the Joule heating rate in the northern hemisphere. Thick lines show the data (courtesy of G. Lu, NCAR/HAO), and thin lines show the model results. As expected, there is virtually no geomagnetic activity in the model, i.e., the modeled CL index never drops below -300

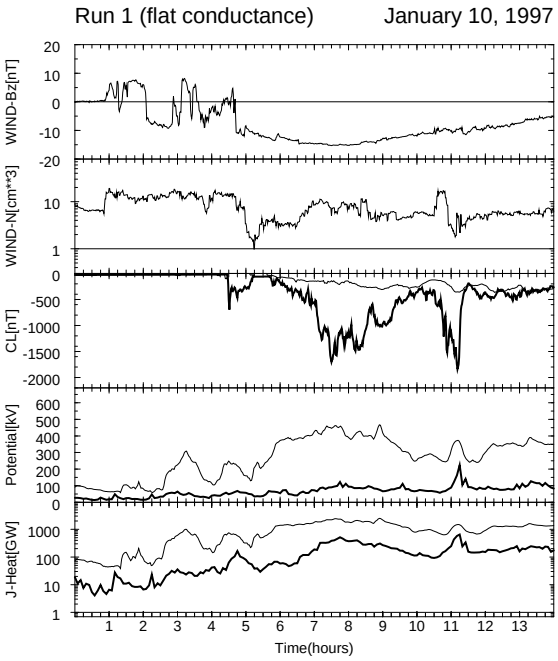

Figure 2. Simulation results for run 1 (flat ionospheric conductance) for January 10, 1997. From top to bottom: IMF B_z; solar wind number density; Canopus CL index; cross polar cap potential; and Joule heating rate. In the lower 3 panels thin lines are for the model results, thick lines are for the data.

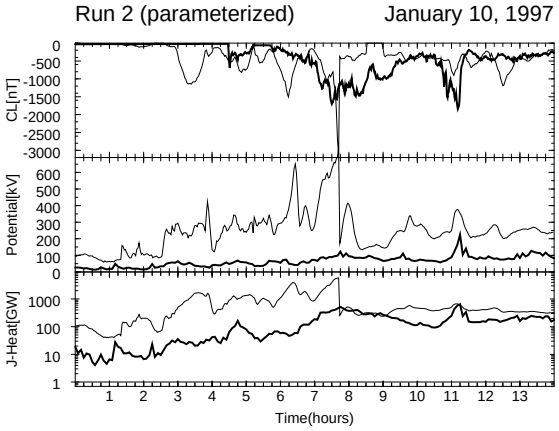

Figure 3. Like Figure 2, but for run 2.

nT, despite the fact that the Canopus values reach -1800 nT. The modeled polar cap potential is very high compared to the AMIE result and consequently the Joule heating rate is almost an order of magnitude larger than the AMIE estimate. In view of earlier results [*Raeder et al.*, 1998] this is also expected and is discussed in more detail below.

Figure 3 shows the results from run 2, where we used a parameterized conductance model [see *Raeder et al.*, 1998, 2001, for details] in lieu of CTIM. The modeled CL index is considerably improved over the case with flat conductance and shows activity levels that are comparable to the observed ones. However, the model also shows several activations that are not real. The potential values are at times somewhat lower compared to run 1, but at other times even higher and reach occasionally 600 kV, which is several times the AMIE estimate. Similarly, the model overestimates the Joule heating rate by about one order of magnitude most of the time.

Results from the fully coupled model are shown in Figure 4. It is immediately evident that the coupled model reproduces the electrojet activity (as measured by CL) more faithfully than the simpler models. The model potential is still considerably higher than the AMIE estimate, however, the differences in the Joule heating rate are less for this model than for the other two models. In the fourth panel of Figure 4 we also show the integrated electron precipitation energy flux over the northern hemisphere and compare it with earlier experimental estimates [*Lu et al.*, 1998]. The energy input produced by the model is slightly less than the data, but generally agrees fairly well with the observations, except during the activation around 1100 UT.

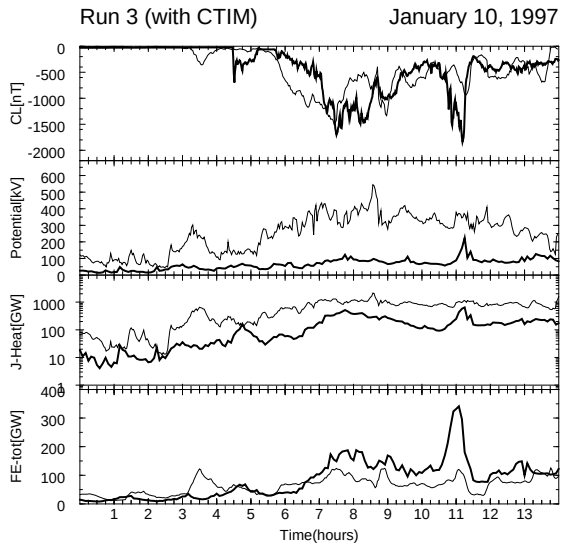

Figure 4. Like Figure 3, but for run 3. In addition, the fourth panel shows the energy flux of precipitating electrons in the northern hemisphere.

6. DISCUSSION AND SUMMARY

Clearly, the coupled model produces a significantly better response than either run 1 or run 2. The main reason appears to be that the self-consistently and from first principles computed ionospheric conductance distribution is far more realistic than either a flat conductance model or simple parameterization. The flat conductance model eliminates any asymmetries and the effects of Hall conductance (uniform Hall conductance falls out of the potential equation), and thus is not expected to yield a realistic response to magnetospheric input.

Figure 5 shows the comparison of the Pedersen (left column) and Hall (right column) conductance from run 2 (parameterized conductances, top row) and from run 3 (CTIM conductances, bottom row). These snapshots were taken at 0800 UT, that is during a period of strong geomagnetic activity. The differences between the two conductance models are significant. Generally, the parameterized model produces a larger Hall conductance but a smaller Pedersen conductance. The empirical model also skews the conductance pattern towards the evening sector and produces very low conductance values in the morning sector, that is between 0600 and 1200 magnetic local time (MLT). Furthermore, the empirical model has very large north-south gradients, in particular in the nightside and in the Hall conductance. CTIM, on the other hand produces much weaker gradients, and in that model moderately large (a few Siemens) conductance values are also seen at lower latitudes (below 60°) in the nightside.

The large nightside conductance gradient and the morningside conductance gap appear to be the main reason for the excessive potential values and their erratic jumps in run 2. The strong gradient must be associated with a strong field-aligned current, a strong ionospheric electric field, or both. If the magnetosphere does not supply an adequate field-aligned current, a strong electric field across the gradient inevitably develops. The magnetosphere responds to that electric field and eventually sets up a field-aligned current that reduces this electric field (note that, if the magnetospheric response were of the opposite sense an instability would develop). However, the magnetospheric response is not necessarily a perfect match nor does it occur instantaneously. Thus, the system switches erratically between different states. Although such processes may indeed occur in nature – evident by the rapidly time-varying aurora – the resolution of our model is by far not sufficient to capture these processes at their correct scales. On the other hand, the CTIM conductance is much smoother and apparently much closer to reality than the empirical model. Although it still produces a far too large cross-polar-cap potential the ground perturbations match exceptionally well with the observations. This suggests that the Hall currents in the model are roughly correct but that the Pedersen currents deviate from reality to a larger extent. Unfortunately, neither the ionospheric currents, nor the ionospheric conductances can be measured directly, and thus we have to rely on indirect constraints, like ground magnetic perturbations, to assess and improve the model.

Despite the improvements brought by CTIM the high cross-polar-cap potential in the model remains a critical issue. Such discrepancy has been found in earlier studies [*Raeder et al.*, 1998] and is also evident in other models [*Fedder et al.*, 1998; *Hill and Toffoletto*, 1998; *Peroomian et al.*, 1998]. Possible causes are discussed in [*Raeder et al.*, 1998] and include reconnection rates in the MHD model that are too high, and the lack of adequate region-2 currents in the model. Based on the results presented here we can now almost certainly rule out inaccuracies of the ionospheric conductance. More detailed comparisons with data, for example with directly measured FACs, are required to find the cause of this discrepancy.

In summary, we have presented the first global, self-consistent, fully electrically coupled, magnetosphere–ionosphere–thermosphere model. Initial results from this model for the January 10, 1997 geomagnetic storm are encouraging, and yield in particular a much more realistic ionospheric response as compared with the previous magnetosphere model that relied on parameterizations for the ionospheric conductance.

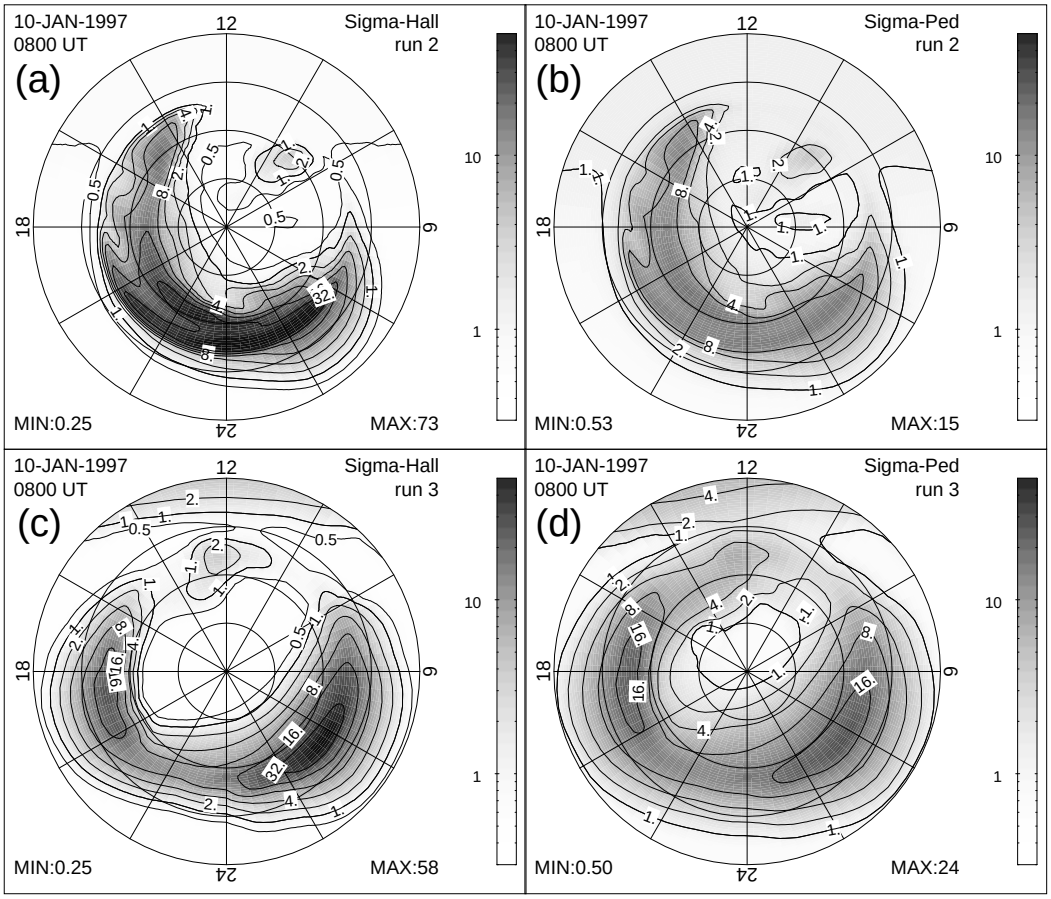

Figure 5. Conductance patterns in the northern polar cap between 50° magnetic latitude and the geomagnetic pole at 0800 UT on January 10, 1997: a) Hall conductance for run 2, b) Pedersen conductance for run 2, c) Hall conductance for run 3, d) Pedersen conductance for run 3. Conductance values are given in Siemens and contour-lines are spaced by a factor of 2.

Acknowledgments.

We thank Gang Lu (NCAR/HAO) for providing the AMIE results for this event. The research at UCLA was supported by NSF grants ATM-97-13449 and ATM-98-01937. YW was supported by LLNL grant ICSR-99-008. Computations were performed on the IBM-SP2 of the San Diego Supercomputer Center and the SGI-Origin2000 at the National Center for Supercomputer Applications. IGPP publication 5477. The Editor would like to thank the reviewers of this manuscript.

References

Evans, C. R., and J. F. Hawley, Simulation of magnetohydrodynamic flows: A constrained transport method, *Astrophys. J.*, *332*, 659, 1988.

Fedder, J. A., S. P. Slinker, and J. G. Lyon, A comparison of global numerical simulation results to data for the January 27-28, 1992, geospace environment modeling challenge event, *J. Geophys. Res.*, *103*, 14799, 1998.

Fox, G. C., M. A. Johnson, G. A. Lyzenga, S. W. Otto, J. K. Salmon, and D. W. Walker, *Solving Problems on Concurrent Processors*, Prentice Hall, Englewood Cliffs, N.J., 1988.

Fox, N. J., M. Peredo, and B. J. Thompson, Cradle to grave tracking of the January 6-11, 1997 Sun-Earth connection event, *Geophys. Res. Lett.*, *25*, 2461, 1998.

Fukushima, N., Equivalence in ground magnetic effect of Chapman-Vestine's and Birkeland-Alfven's current systems for polar magnetic storms, *Rep. Ionos. Space Res. Jpn.*, *22*, 219, 1969.

Fukushima, N., Generalized theorem for no ground magnetic effect of vertical currents connected with Pedersen currents in the uniform conducting ionosphere, *Rep. Ionos. Space Res. Jpn.*, *30*, 35, 1976.

Fuller-Rowell, T. J., D. Rees, S. Quegan, R. J. Moffett, M. V. Codrescu, and G. H. Millward, A coupled thermosphere-ionosphere model (CTIM), in *STEP Report*, edited by R. W. Schunk, p. 217, NOAA/NGDC, Boulder, Colorado, Scientific Committee on Solar Terrestrial Physics (SCOSTEP), 1996.

Gombosi, T. I., D. L. DeZeeuw, C. P. T. Groth, K. G. Powell, and P. Song, The length of the magnetotail for northward IMF: Results of 3D MHD simulations, in *Phys. Space Plasmas (1998)*, edited by T. Chang, and J. R. Jasperse, vol. 15, p. 121, Cambridge, Mass., 1998.

Goodrich, C. C., J. G. Lyon, M. Wiltberger, R. E. Lopez, and K. Papadopoulos, An overview of the impact of the January 10-11, 1997, magnetic cloud on the magnetosphere via global MHD simulation, *Geophys. Res. Lett.*, *25*, 2537, 1998.

Harten, A., and G. Zwas, Self-adjusting hybrid schemes for shock computations, *J. Comput. Phys.*, *9*, 568, 1972.

Hill, T. W., and F. R. Toffoletto, Comparison of empirical and theoretical polar cap convection patterns for the January 1992 GEM interval, *J. Geophys. Res.*, *103*, 14811, 1998.

Hirsch, C., *Numerical Computation of Internal and External Flow*, vol. II, John Wiley, New York, 1990.

Janhunen, P., T. I. Pulkkinen, and K. Kauristie, Auroral fading in ionosphere-magnetosphere coupling model: Implications for possible mechanisms, *Geophys. Res. Lett.*, *22*, 2049, 1995.

Kamide, Y., A. D. Richmond, and S. Matsushita, Estimation of ionospheric electric fields, ionospheric currents, and field-aligned currents from ground magnetic records, *J. Geophys. Res.*, *86*, 801, 1981.

Kelley, M. C., *The Earth's Ionosphere*, Academic Press, New York, 1989.

Kennel, C. F., and H. E. Petschek, Limit on stably trapped particle fluxes, *J. Geophys. Res.*, *71*, 1, 1966.

Lu, G., et al., Global energy deposition during the January 1997 magnetic cloud event, *J. Geophys. Res.*, *103*, 11685, 1998.

Lyon, J. G., R. E. Lopez, C. C. Goodrich, M. Wiltberger, and K. Papadopoulos, Simulation of the March 9, 1995, substorm: Auroral brightening and the onset of lobe reconnection, *Geophys. Res. Lett.*, *25*, 3039, 1998.

Lyons, L. R., D. Evans, and R. Lundin, An observed relation between magnetic field aligned electric fields and downward electron energy fluxes in the vicinity of auroral forms, *J. Geophys. Res.*, *84*, 457, 1979.

Ogino, T., A three dimensional MHD simulation of the interaction of the solar wind with the Earth's magnetosphere: The generation of field aligned currents, *J. Geophys. Res.*, *91*, 6791, 1986.

Peroomian, V., L. R. Lyons, M. Shultz, and D. C. Pidmore-Brown, Comparison of assimilative mapping and source surface model results for magnetospheric events of January 27 to 28, 1992, *J. Geophys. Res.*, *103*, 14819, 1998.

Raeder, J., Modeling the magnetosphere for northward interplanetary magnetic field: Effects of electrical resistivity, *J. Geophys. Res.*, *104*, 17357, 1999.

Raeder, J., et al., Global simulation of the geospace environment modeling substorm challenge event, *J. Geophys. Res.*, *106*, 381, 2001.

Raeder, J., J. Berchem, and M. Ashour-Abdalla, The Geospace Environment Modeling grand challenge: Results from a Global Geospace Circulation Model, *J. Geophys. Res.*, *103*, 14787, 1998.

Richmond, A. D., and Y. Kamide, Mapping electrodynamic features of the high latitude ionosphere from localized observations, *J. Geophys. Res.*, *93*, 5741, 1988.

Richmond, A. D., and R. G. Roble, Electrodynamic effects of thermospheric winds for the NCAR thermospheric general circulation model, *J. Geophys. Res.*, *92*, 12365, 1987.

Robinson, R. M., R. R. Vondrak, K. Miller, T. Dabbs, and D. Hardy, On calculating ionospheric conductances from the flux and energy of precipitating electrons, *J. Geophys. Res.*, *92*, 2565, 1987.

Roble, R. G., and E. C. Ridley, A Thermosphere - Ionosphere - Mesosphere - Electrodynamics General Circulation Model (TIME-GCM): Equinox solar cycle minimum simulations (30-500 km), *Geophys. Res. Lett.*, *21*, 417, 1994.

Rostoker, G., J. C. Samson, F. Creutzberg, T. J. Hughes, D. R. McDiarmid, A. G. McNamara, A. Vallace-Jones, D. D. Wallis, and L. L. Cogger, CANOPUS - A ground based instrument array for remote sensing the high latitude ionosphere during the ISTP/GGS program, *Space Sci. Rev.*, *71*, 743, 1995.

Slinker, S. P., J. A. Fedder, J. Chen, and J. G. Lyon, Global MHD simulation of the magnetosphere and ionosphere for 1930-2330 ut on November 3, 1993, *J. Geophys. Res.*, *103*, 26243, 1998.

Spann, J. F., M. Brittnacher, R. Elsen, G. A. Germany, and G. K. Parks, Initial response and complex polar cap structures of the

aurora in response to the January 10, 1997 magnetic cloud, *Geophys. Res. Lett.*, *25*, 2577, 1998.

Tanaka, T., Generation mechanisms for magnetosphere-ionosphere current systems deduced from a three-dimensional MHD simulation of the solar wind-magnetosphere-ionosphere coupling processes, *J. Geophys. Res.*, *100*, 12057, 1995.

Weimer, D. R., D. A. Gurnett, C. K. Goertz, J. D. Menietti, J. L. Burch, and M. Sugiura, The current – voltage relationship in auroral current sheets, *J. Geophys. Res.*, *92*, 187, 1987.

Winglee, R. M., and J. D. Menietti, Auroral activity associated with pressure pulses and substorms: A comparison between global fluid modeling and Viking UV imaging, *J. Geophys. Res.*, *103*, 9189, 1998.

J. Raeder, Institute of Geophysics and Planetary Physics, University of California, 405 Hilgard Ave, Los Angeles, CA 90095-1567. (e-mail: jraeder@igpp.ucla.edu)

Y. Wang, Department of Earth and Space Sciences, University of California, 405 Hilgard Ave, Los Angeles, CA 90095-1567. (e-mail: ylwang@igpp.ucla.edu)

T. J. Fuller-Rowell, NOAA Space Environment Center R/E/SE, 325 Broadway, Boulder, CO 80303. (e-mail: tjfr@sec.noaa.gov)

This preprint was prepared with AGU's LaTeX macros v4, with the extension package `AGU++' by P. W. Daly, version 1.5a from 1996/10/09.